Organic & Biomolecular Chemistry

Accepted Manuscript

This article can be cited before page numbers have been issued, to do this please use: D. M. Miles-Barrett, A. R. Neal, C. Hand, J. R.D. Montgomery, I. Panovic, O. S. Ojo, C. S. Lancefield, D. B. Cordes, A. Slawin, T. Lebl and N. J. Westwood, *Org. Biomol. Chem.*, 2016, DOI: 10.1039/C6OB01915C.

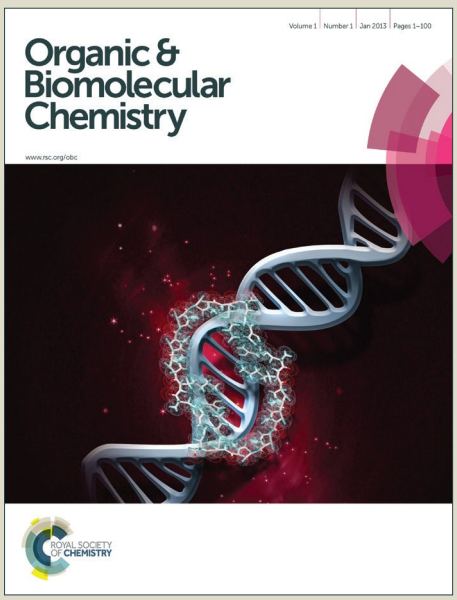

ROYAL SOCIETY OF CHEMISTRY

www.rsc.org/obc

View Article Online
DOI: 10.1039/C6OB01915C

Journal Name

ARTICLE

The synthesis and analysis of lignin-bound Hibbert ketone structures in technical lignins

§Received 00th January 20xx,
Accepted 00th January 20xx

DOI: 10.1039/x0xx00000x

www.rsc.org/

D. M. Miles-Barrett†, A. R. Neal†, C. Hand, J. R. D. Montgomery, I. Panovic, O. S. Ojo, C. S. Lancefield, D. B. Cordes, A. M. Z. Slawin, T. Lebl and N. J. Westwood[a]*

Understanding the structure of technical lignins resulting from acid-catalysed treatment of lignocellulosic biomass is important for their future applications. Here we report an investigation into the fate of lignin under acidic aqueous organosolv conditions. In particular we examine in detail the formation and reactivity of non-native Hibbert ketone structures found in isolated organosolv lignins from both Douglas fir and beech woods. Through the use of model compounds combined with HSQC, HMBC and HSQC-TOCSY NMR experiments we demonstrate that, depending on the lignin source, both S and G lignin-bound Hibbert ketone units can be present. We also show that these units can serve as a source of novel mono-aromatic compounds following an additional lignin depolymerisation reaction.

Introduction

Lignin, a core component of the cell wall, is thought to be the most recalcitrant and intractable biopolymer in lignocellulosic biomass. The ability to identify and assess the reactivity of the different structural units within this biopolymer is a fundamental aspect of understanding lignin's structure and advancing methods for its selective depolymerisation to generate renewable chemical feedstocks.[1–9] Recently, interest has increased in protocols that liberate lignin from biomass without causing large structural changes to the lignin (*e.g.* mild organosolv methods).[4,10–14] Many of these approaches have developed from the acidolysis methods examined in the 1940-70s.[15–19] Whilst progress on mild lignin isolation protocols continues, it is clear that structural modification of the lignin will always occur to some extent and that the induced changes require more detailed study.

The Hibbert ketones (HKs), named after their discoverer Harold Hibbert,[16–18,20] encompass a series of keto-containing structures that are formed on acidolysis of lignin (Figure S1).[16–18,20] The family includes ketones **1** and **2** (Scheme 1A)[19] which are likely formed from lignin as shown in Scheme 1B. The acidolysis reaction begins with (i) protonation of the benzylic hydroxyl groups on adjacent β-O-4 units leading to (ii) the formation of carbocation/quinone methide intermediates.[19]

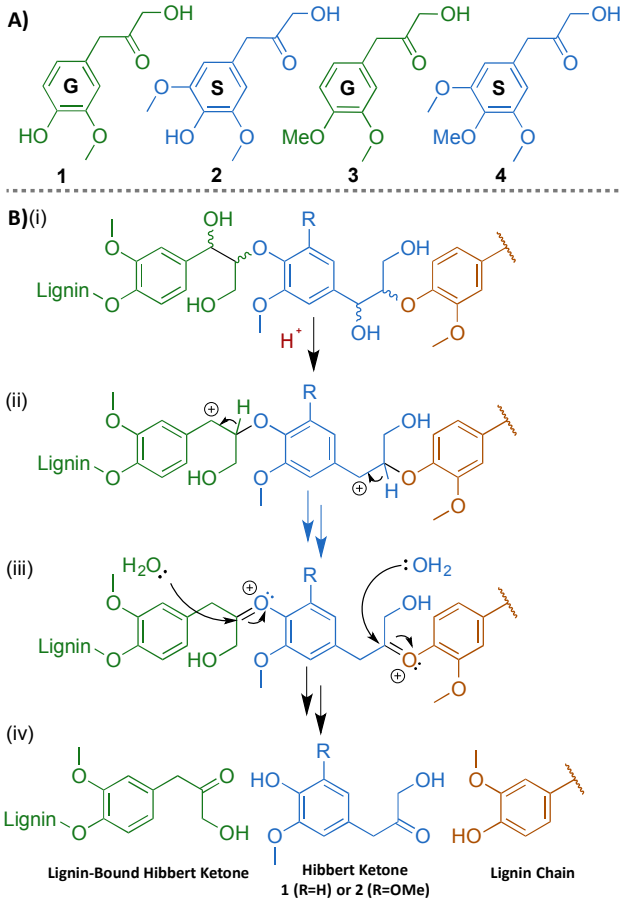

Scheme 1A: Guaiacyl (G) **1** and sinapyl (S) **2** Hibbert ketones and their methylated analogues **3** and **4** were synthesised in this study. **1B**: Proposed mechanism for generation of HK **1** or **2** and a lignin-bound Hibbert ketone (LBHK) structure on acidolysis of two adjacent β-O-4 units in lignin. Models **3** and **4** mimic the LBHK structures. For more information, see ESI Scheme S1.

[a] *School of Chemistry and Biomedical Sciences Research Complex, University of St. Andrews and EaStCHEM, St Andrews, Fife, Scotland, KY16 9ST (UK)*
** E-mail: njw3@st-andrews.ac.uk*

† These authors contributed equally.

Electronic Supplementary Information (ESI) available: Detailed synthetic procedures and data for novel compounds. See DOI: 10.1039/x0xx00000x

View Article Online
DOI: 10.1039/C6OB01915C

Subsequent loss of a proton is followed by hydrolysis of the resulting enol ethers (not shown) to give the labile oxonium ions shown in (iii). Attack by H_2O and collapse of the resulting hemi-ketals releases HK **1** or **2** (iv) (blue structure). Interestingly, this process as drawn should also result in formation of a lignin-bound Hibbert ketone structure (LBHK, green) from the second β-O-4 unit (from a C3-C3 degradation pathway, see Schemes S2-S3 for other possible pathways).

Whilst the identification of HKs **1** and **2** during lignin acidolysis is well-known,[19] the formation of the LBHK unit is less well studied with only partial assignments in 2D HSQC spectra being present in the literature to the best of our knowledge.[21–23] Here we initially address this issue through the synthesis of **3** and **4**, models of the LBHK structures. Previous syntheses of these types of compounds have included Hibbert's original route to **1** from homoveratric acid involving the use of diazomethane.[18] Lundquist has also reported a synthesis of **1** from an unprotected triol precursor.[19] The most recent report in this area by Dalla *et al*. involved reaction of a silyl-protected Wittig reagent with the required aldehyde followed by LAH reduction to give **3**.[24]

Here we report a synthesis of non-phenolic and phenolic Hibbert ketones (**1**-**4**) in both the G and S series. A detailed NMR comparison of lignin generated from both soft- and hardwoods with **3** and **4** demonstrates that LBHK structures are indeed present and are available for study by 2D HSQC and HMBC methods. In addition, the availability of compounds **1**-**4** enables studies on the reactivity of the LBHK structures to be carried out. Studying reactions on lignin model compounds (e.g. β-O-4, β-5, β-β) prior to testing them on lignin has allowed for recent breakthroughs in several depolymerisation procedures.[3,25–27] In particular, acid-induced depolymerisations (e.g. formic acid,[25] triflic acid[3]) that give high weight % yields of C2[3] and C3[25] monomers have been developed. To date, these procedures have not been studied in the context of LBHK structures (e.g. **1**-**4**), despite the fact that they are often present within the starting lignins or are generated as the depolymerisation reaction progresses.

Results and Discussion

Synthesis of Model Compounds

Our approach to non-phenolic LBHK models (**3** and **4**) began with the addition of vinylmagnesium bromide to 3,4-dimethoxybenzaldehyde (**5**), followed by dihydroxylation of the intermediate olefin to give triol **6** (39% yield over 2 steps, d.r. 3.0:1). Acidolysis of **6** in 2M HCl/dioxane (1:9)[19] gave the desired ketone **3** in 45% yield after purification. The same approach was applied to 3,4,5-trimethoxybenzaldehyde (**7**) to give triol **8** in comparable yield (36% over 2 steps, d.r. 2.6:1). Again, acidolysis of **8** in 2M HCl/dioxane (1:9) gave the required ketone **4** in 37% yield. The HKs **1** and **2** were also synthesised as these structures would be released on depolymerisation of lignin samples and may prove useful as a versatile building block in synthesis (Scheme 2(ii)).

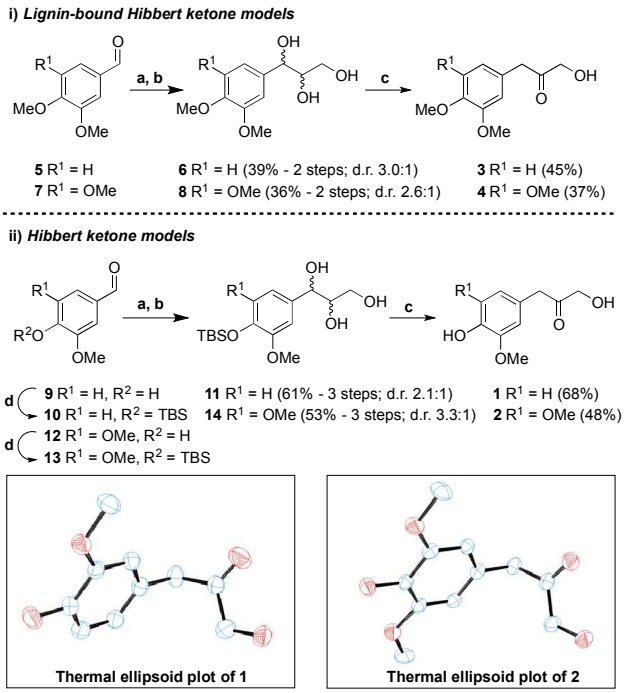

Scheme 2: Synthetic routes to (i) lignin-bound HK models and; (ii) authentic samples of the Hibbert ketones. Reaction conditions: (**a**) vinylmagnesium bromide (1.1-1.2 eq.), THF, 0°C - r.t. 1 h. (**b**) OsO_4, NMO (1.5-1.7 eq.), THF/ H_2O (9:1), r.t. 16 hrs. (**c**) 1,4-dioxane: 2M HCl (9:1), 0.5 – 1 h. (**d**) TBS-Cl (1.2 eq.), imidazole (2.0 eq.), DMAP (5 mol%) DCM, r.t., 1 - 2 hrs. Thermal ellipsoid plot representations of **1** and **2** are shown at 50% ellipsoid probability, hydrogens omitted for clarity.[28]

Initially, TBS protection of vanillin (**9**) was performed to give **10**. Treatment of **10** with vinylmagnesium bromide and dihydroxylation gave triol **11** (61% over 3 steps, d.r. 2.1:1) in an analogous manner to the formation of **6** and **8**. Acidolysis of triol **11** led directly to ketone **1** (in 68% yield) with acid mediated silyl deprotection observed. X-ray crystallographic analysis confirmed the successful synthesis of ketone **1**.[28] Finally, TBS protection of syringaldehyde (**12**) gave **13**. The addition of vinylmagnesium bromide to **13** and subsequent dihydroxylation gave triol **14** (53% over 3 steps, d.r. 3.3:1). Again, acidolysis of **14** led to the desired ketone **2** (48% yield) and this structure was confirmed by X-ray crystallographic analysis.[28] Having successfully synthesised ketones **1**-**4**, our focus turned to using these compounds in the analysis of the Hibbert ketone structure in lignin.

Identification of Lignin-Bound Hibbert Ketone units in Softwood and Hardwood Lignins

Two lignins, Douglas Fir (DF) and beech were isolated using a dioxasolv extraction method (0.2M HCl in 1,4-dioxane, 1 hour at reflux).[27] Analysis of the 2D HSQC NMR overlays of DF and beech lignin with G- and S-LBHK models **3** and **4** respectively enabled assignment of all the relevant cross-peaks (Figure 1). The α-protons in both **3** and **4** can be assigned as a distinctive peak at δ_C/δ_H 44.6/ 3.64 ppm (Figures 1A & 1C) in a

View Article Online
DOI: 10.1039/C6OB01915C

region cut from most reported lignin NMR spectra.[21] The γ-protons, δ_C/δ_H 67.6/ 4.17 ppm (Figures 1A & 1C), are located above the β-β cross-peaks and the α- and γ-cross-peaks are, to the best of our knowledge, the only HK related peaks currently assigned in the literature.[21,22] From the analysis of the aromatic regions (Figures 1B & 1D), the G6-LBHK aromatic cross-peak can be assigned at δ_C/δ_H 122.1/ 6.65 ppm and is notably more shielded in the carbon dimension than the $G5/6_{native}$ (native to the protolignin structure) cross-peak located at δ_C/δ_H 119.5/ 6.8 ppm (Figure 1B). The G_2-LBHK cross-peak can be assigned at δ_C/δ_H 113.5/ 6.75 ppm and the G_5-LBHK (δ_C/δ_H 112.8/ 6.88 ppm) overlaps with the $G2_{native}$ cross-peak (Figure 1B). Interestingly, the S2/S6-LBHK cross-peak is in a region usually assigned as 'condensed' lignin structures (δ_C/δ_H 107.4/ 6.52 ppm, circled in Figure 1D). It is unlikely the intensity of this cross-peak corresponds solely to S-LBHK content, but explains it partially.

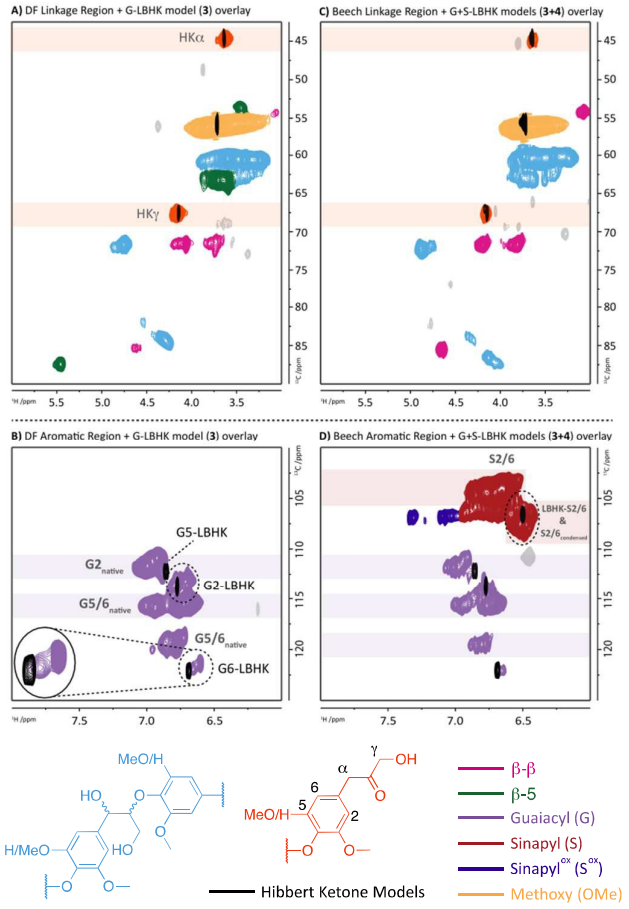

Figure 1: 2D HSQC NMR analysis (700 MHz, d_6-DMSO) of: **A)** DF linkage region overlaid with spectrum from G-LBHK model **3**; **B)** Beech linkage overlaid with spectrum from S-LBHK model **4**; **C)** DF aromatic region overlay with spectrum from **3**; **D)** Beech aromatic region overlay with spectra from **3** and **4**. See ESI Figure S2 for further detail. Circled peaks are discussed in text.

Analysis of the Effect of acid concentration on Lignin Structure

Isolation of lignin using different acid pretreatment conditions would be expected to influence the LBHK content. The β-O-4 linkage is the only linkage in lignin that can give rise to a LBHK structure on cleavage. Therefore, if pretreatment conditions were used that led to reaction (and hence loss) of β-O-4 units it would be expected that a proportional increase in LBHK content would occur (note: every time two adjacent β-O-4 units are both cleaved one molecule of HK **1** or **2** and one LBHK unit could be formed (Scheme 1B)). Loss of LBHK units may occur due to equilibration to other isomeric HKs over time (ESI Figure S1). To examine changes in the extent of LBHK formation as a function of acid concentration, dioxasolv extractions were conducted on two woods (DF and beech) using different acid concentrations. The soluble lignin component of the samples were analysed by 2D HSQC NMR to establish the effects of changes in the pretreatment conditions on linkage content.

On analysis of lignins obtained from DF wood at increasing acid concentrations (Table 1A), several observations were noted: (i) the isolated yields of lignin increased with acid concentration, presumably due to release of additional lignin from the hemicellulose/cellulose components; (ii) the amounts of the β-β and β-5 linkages remained relatively fixed, suggesting that these units are not acid sensitive and (iii) as the acid concentration increased, the β-O-4 content decreased with the LBHK content increasing by an analogous amount.

Analysis of the beech wood derived lignin as a function of increasing acid concentrations (Table 1B) led to the following observations; (i) as seen with DF, the isolated lignin yields increased and the β-β and β-5 content remained almost constant (although evidence that the epimerisation of the β-β had occurred at higher acid concentration was obtained, ESI Figure S3); (ii) in contrast to DF, whilst the β-O-4 content again decreased as the acid concentration increased, the apparent increase in LBHK units was much lower than expected and was not analogous to the β-O-4 loss (Table 1B) This may have been because β-O-4 units are more prevalent in hardwoods than in softwoods (60-62% for hardwoods; 45-50% for softwoods).[2] This increases the probability that two or more β-O-4 units are present in succession in hardwoods. This therefore increases the chance that consecutive β-O-4 units are cleaved releasing HKs **1** and **2** and reducing the LBHK content; (iii) the S:G ratio (hardwoods are usually enriched in S units[2]) increased in favour of the S units as the acid concentration increased. Possible explanations for this include: (a) the G aromatic units are retained but have increasingly reacted at the C5 position as acid concentration was increased (the lignin is increasingly condensed) and/or (b) that the G unit-rich S1 layer of the cell wall (in hardwoods[29]) is preferentially extracted at lower acid concentrations whereas the S2 and S3 layers of the cell wall (which are richer in S units than the S1 layer in hardwoods[29]) are also extracted at higher acid concentrations.

View Article Online
DOI: 10.1039/C6OB01915C

Table 1: Dioxasolv extractions to give **A**) softwood DF lignin and **B**) hardwood beech lignin.

A) Softwood Douglas Fir	HCl Concentration / M	Isolated Lignin / wt. % *	Per 100 C_9 Units β-O-4	β–β	β–5	LBHK
	0.05	2.3	34	5	14	8 (42)
	0.2	4.4	28	6	15	18 (46)
	0.4	6.9	24	6	15	23 (47)

B) Hardwood Beech	HCl Concentration / M	Isolated Lignin / wt. % *	S:G ratio	Per 100 C_9 Units β-O-4	β–β	β–5	LBHK
	0.05	1.2	1.8: 1	53	8	5	3 (56)
	0.2	9	3.3: 1	40	11	3	7 (47)
	0.4	11.2	3.6: 1	32	10	3	10 (42)

All extractions were conducted on a 10 g scale. Number *per* 100 C9 units was calculated based on integrations of 2D HSQC NMR cross-peaks (see ESI Figures S4-S5). For standard error analysis of 3 repetitions, see ESI Tables S3-S4. To assess possible concerns over the use of 2D HSQC NMR analysis for linkage quantification (as end-groups (e.g. LBHKs) are suggested to be over-represented within lignin 2D HSQC NMR spectra[2]), NMR experiments were conducted to assess the dependence of cross peaks integral values on T_1 relaxation times (ESI Table S5-S6). In these experiments, the number *per* 100 C9 units was found to increase for β-O-4 units and decrease for β-5, β–β and LBHK units when the D_1 time was extended from 1s to 15s. Values in parentheses = total number of β-O-4 + LBHK units. The results presented here should be viewed as semi-quantitative. The quantitative 2D HSQC NMR analysis of lignin can only be obtained using specific pulse sequences.[30] * the reported isolated yields are after Et_2O precipitations (as sequential washings whilst they removed low M_W contaminants, significantly lowered lignin isolated yields (~50% loss) due to partial fractionation of lignin).

GPC elution profiles of the beech lignins showed that the weighted average of the molecular weight (M_w) decreased with increasing acid concentration (ESI Tables S1-S2). This suggests that the increased condensation (see (a) above) does not explain the observed increase in the S:G ratio. In summary, the amount of LBHK units in a particular lignin clearly varies depending on the wood type and pretreatment conditions.

HMBC analysis of dioxasolv lignins

Assessing whether both the S- and the G-lignin-bound Hibbert ketone structures were present in the lignins was difficult by 2D HSQC NMR (Figure 1). This was due to overlap of the aliphatic cross-peaks associated with the two LBHK structures and also because of the overlap between the distinctive S-LBHK aromatic cross-peaks and the S2/6$_{condensed}$ cross-peaks in lignin. To determine whether G-LBHK and/or S-LBHK structures were present in our lignins, HMBC analysis therefore had to be used (Figure 2). An indication that this experiment could be used came from the fact that the cross-peak corresponding to the β-carbonyl carbon (δ_C 208.6 ppm) in the G-LBHK model **3** could be observed due to its coupling to the LBHK α-proton (δ_H/δ_C 3.63-3.67/44.6 ppm) (Figure 2A and figure legend for labelling). The β-carbonyl carbon in **3** also coupled with the G1, G2 and G6 protons (Figure 2A). Comparison of the cross-peaks in **3** with those observed in the same region of the DF lignin HMBC spectrum (Figure 2B) confirmed that the G-LBHK structure was present in the lignin sample (Figure 2C for overlay of HMBC spectra). As expected, no signals corresponding to the S-LBHK structure were observed in this softwood-derived lignin (softwoods are very G-rich, *vide infra*).

HMBC analysis of the S-LBHK model **4** (Figure 2D) revealed that the S1 and S2/6 cross-peaks were distinguishable from the corresponding G-aromatic cross-peaks in the G-LBHK model **3**. An overlay of the HMBC spectrum of **4** (Figure 2D) with that of the beech lignin (Figure 2E) showed that the S1 and S2/6 aromatic cross-peaks were present in both spectra (Figure 2F). Cross-peaks that overlapped with those of model **3** were also observed in the beech lignin analysis. This confirmed that *both* G- and S-LBHK structures were formed during acidolysis of the hardwood.[§] In the next phase of the project we decided to investigate whether chemical modification of the LBHK structures in DF lignin could be achieved.

Reaction of LBHKs and analysis by 2D HSQC-TOCSY NMR

To investigate the reactivity of the lignin-bound Hibbert ketone structures the following experiment was proposed (Figure 3). Reduction of our sample of DF Lignin with $NaBH_4$ would be expected to convert any ketones to the corresponding alcohols (including in the LBHK structures) to give reduced DF lignin (referred to here as DFRD). It was decided to use a 2D HSQC-TOCSY NMR experiment to assess if reduction of the LBHK units had been successful as this experiment enables complete spin systems to be observed. Thirteen weight percent of $NaBH_4$ in THF: H_2O (2:1) at room temperature was used to convert a DF lignin sample (prepared using 0.4 M HCl, Table 1A) to the corresponding DFRD.

To aid structural assignment model **3** was also reduced by $NaBH_4$ to give a sample of **15** (Figure 3). 2D-HSQC-TOCSY NMR analysis of **15** (Figure 3A for the set of cross-peaks at δ_C 65.7 ppm) showed that TOCSY transfer from γ–CH to α, β and β/γ-OH protons had occurred. Analogous cross peaks were present in the 2D HSQC-TOCSY NMR spectrum of the DFRD lignin (Figure 3B) and excellent overlap of the two sets of cross-peaks was observed (Figure 3C) confirming the reduction of the carbonyl group in the LBHK units had occurred as predicted.

View Article Online
DOI: 10.1039/C6OB01915C

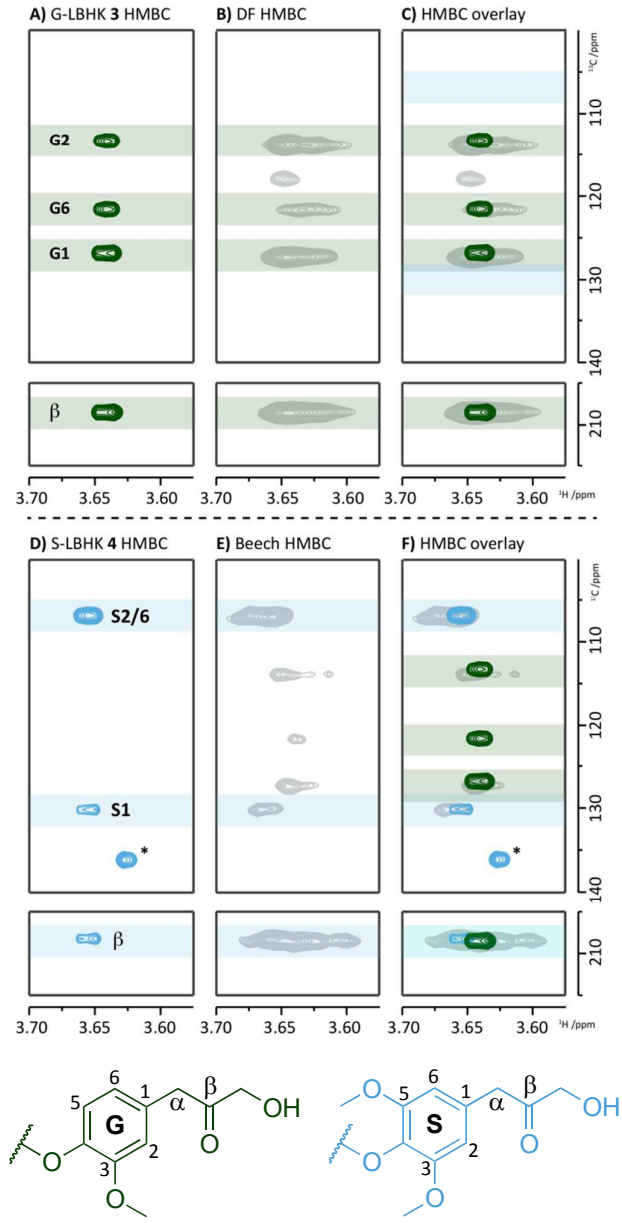

Figure 2: 2D HMBC NMR analysis (700 MHz, d_6-DMSO) of: **A**) G-LBHK **3**; **B**) DF lignin (0.4M dioxasolv); **C**) HMBC overlay of A and B; **D**) S-LBHK **4**; **E**) Beech lignin (0.4M dioxasolv); **F**) HMBC overlay of A, D and E. Peak at δ_C/δ_H 3.65/117.9 in DF lignin (**B** and **C**) corresponds to C5 of a G-LBHK unit (green). *Peak at δ_C/δ_H 136.1/3.63 ppm corresponds to ^{13}C3/5 observed from ^{1}H 3.63 ppm of *p*-OMe of S-LBHK model **4** (blue). For ^{13}C numbering, see annotated figures above. Blue bands in **C** emphasise the lack of S-LBHK present in the DF lignin. For full data see ESI Figures S11-S12.

In addition, comparison of the 2D HSQC NMR of **15** with that of the sample of DFRD (ESI Figure S13) supported the view that reaction of the ketone group in the LBHK units had been achieved.

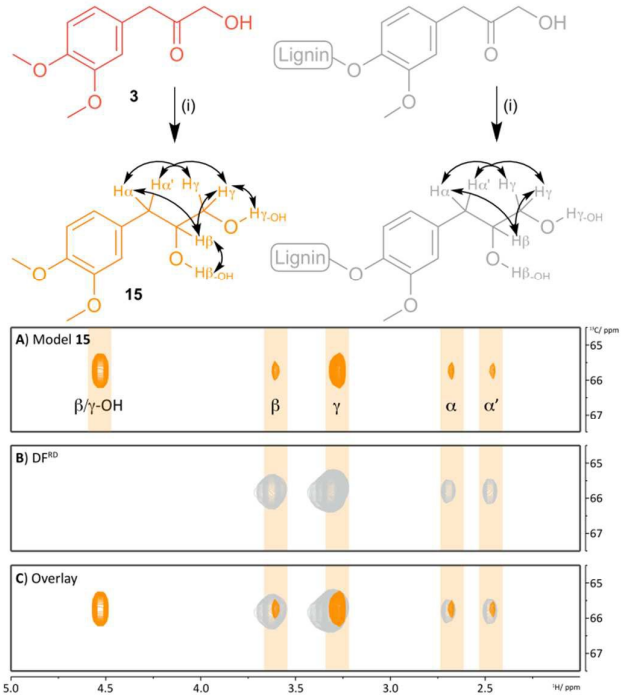

Figure 3: 2D HSQC-TOCSY NMR analysis (700 MHz, d_6-DMSO): expansion of CH-γ cross-peak at ^{13}C 65.7 ppm of: **A)** Model **15** and **B**) DFRD. **C**) Overlay of spectra from A and B. See ESI for acquisition parameters. Reaction conditions: (i) $NaBH_4$, THF: H_2O (2:1), r.t. 16 hours. ESI Figures S14-S15 for full 2D data. Note: the only cross-peak not observed in lignin corresponded to the β/γ-OH. Possible rationalisations for this observation include the expected T_2 relaxation differences in lignin compared to **15** or exchangeability of the -OHs within the lignin sample.

Releasing novel aromatic monomers from LBHK-containing lignins

We have recently reported a method of selectively depolymerising lignin through controlled processing of adjacent β-O-4 units.[27] Here we initially explored whether this methodology (selective oxidation followed by reductive C-O bond cleavage) could be used to cleave the existing LBHK units from the lignin to give the HKs **1**/**2** or derivatives of them. Unfortunately, our protocol was not useful in this case (for preliminary studies see ESI Scheme S4 and Figure S16). Our attention therefore turned to a second depolymerisation methodology we have collaborated on that has been developed by Barta and de Vries *et al*.[3,26a-b]

Barta and de Vries' work has shown that efficient lignin depolymerisation can be achieved by *in situ* trapping of acid (HOTf or M(OTf)$_x$)-generated aldehydes with 1,2-ethanediol to generate predominantly C2 protected acetals (Scheme 3A).[3,26a-b] The generation of acidolysis products derived from intermediates on the minor C3-acidolysis pathway was also observed in this previous work (see ESI Scheme S5).[26a] However, the focus of the original reports[26b] was not on the fate of the LBHK units that were already present in the starting dioxasolv lignins. Here we investigate this issue further through the use of our samples of compounds **1** and **3**. These

View Article Online
DOI: 10.1039/C6OB01915C

studies were then followed by reaction of a lignin containing LBHK units.

Two situations were initially considered. In the first of these, the LBHK unit is attached to an acid-stable linkage. It seemed most likely that the outcome of the reaction with, for example catalytic $Bi(OTf)_3$ and 1,2-ethanediol,[26b] would be that the corresponding lignin-bound ketal would form and no monomer unit would be released (Scheme 3B). In support of this view, successful conversion of model compound **3** to the corresponding ketal **16** was achieved under standard depolymerisation conditions ($Bi(OTf)_3$ (5 wt.%), 1,2-ethanediol (1 eq.), 1,4-dioxane, 140 °C[26b] (Schemes 4A, S6 and Figure S17)).

The second situation occurs when the LBHK unit is attached to an acid-cleavable linkage (Scheme 3C). In this case release of the corresponding Hibbert ketone-derived ketal **17** was expected. This could be achieved either by initial ketal formation whilst the HK unit was attached to the lignin followed by release of **17** or by release of HK **1** followed by ketal formation to give **17**. To explore this further, the reaction of Hibbert ketone **1** with $Bi(OTf)_3$ (5 wt.%) and 1,2-ethanediol was attempted and led to the unexpected generation of dioxene **18** as the major product (Schemes 4B, S7 and Figure S18) with only small quantities of ketal **17** being observed. Isolation of **18** proved possible by chromatography and full structural assignment was carried out (Figure S19). One possible mechanism for the formation of **18** from **1** is shown in Scheme 4C.

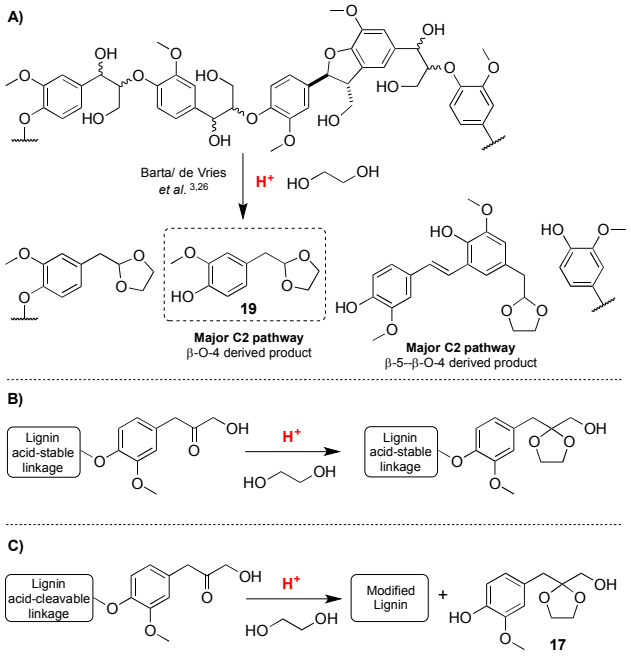

Scheme 3: A) Controlled depolymerisation of lignin under TfOH or $M(OTf)_x$ reactions conditions as previously reported by Barta /de Vries *et al.*[3,26a-b]. Proposed reactivity of the LBHK structure when subjected to $M(OTf)_x$ depolymerisation conditions when the LBHK unit is located adjacent to: **B)** an acid-stable linkage and **C)** an acid-cleavable linker.

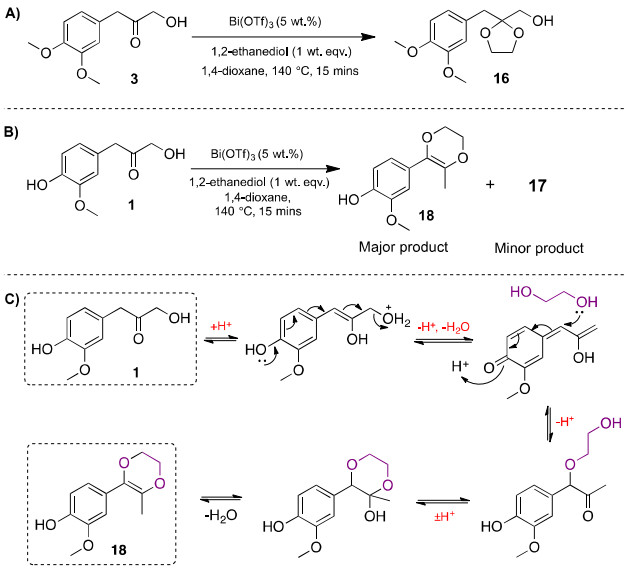

Scheme 4: Reaction of **A)** Model LBHK **3** and **B)** HK **1**, under Lewis-acid-catalysed depolymerisation conditions: Bi(OTf)3 (5 wt. %), ethylene glycol (1 wt. eqv.), 1,4-dioxane, 140 °C, 15 minutes. . **C)** Proposed mechanism for the formation of **18** from **1**. Note: The formation of a small amount of a second product in the reaction with **3** was observed (Figure S17). However, the quantities of this second product were too small to enable definitive structural assignment.

In an attempt to form ketal **17** (rather than **18**) as the major product on reaction of **1**, a screen of different metal triflates was conducted (ESI Table S7 and Figure S20). This study led to a decision to use $Sc(OTf)_3$ (5 wt.%) in the reaction with lignin rather than $Bi(OTf)_3$ as a product distribution of 0.04: 0.77: 0.19 (**1**: **17**: **18**) was obtained on reaction of **1** with $Sc(OTf)_3$ as compared to the 0: 0.15: 0.85 (**1**: **17**: **18**) ratio obtained with $Bi(OTf)_3$ under analogous reaction conditions.*

Treatment of DF lignin with $Sc(OTf)_3$ (5 wt.%) in the presence of 1,2-ethanediol (1 wt. eqv.) in 1,4-dioxane at 140 °C for 15 minutes in a sealed tube was followed, after work-up, by analysis of the low molecular weight fractions using the GC-FID technique (Figure 4). This analysis clearly showed that products **17** and **18** had formed from lignin (by comparison with authentic samples of **17**, r.t: 24.83 mins and **18**, r.t. 23.60 mins, Figures 4B and 4C).

The most likely explanation for the production of **17** and **18** is that they have been released from LBHK structures that were already present in the starting lignin and adjacent to an acid cleavable linkage. In addition, the major product in the lignin-derived sample was acetal **19**, which is known to result from the cleavage of adjacent β-O-4 units within the starting lignin.[26a] It was observed that the ratio of **17**:**18** differed when $Sc(OTf)_3$ was used with lignin as compared to the model studies with **1**.‡ Importantly, however, it was demonstrated that novel lignin-derived aromatics **17** and **18** were formed from lignin in this reaction.

View Article Online
DOI: 10.1039/C6OB01915C

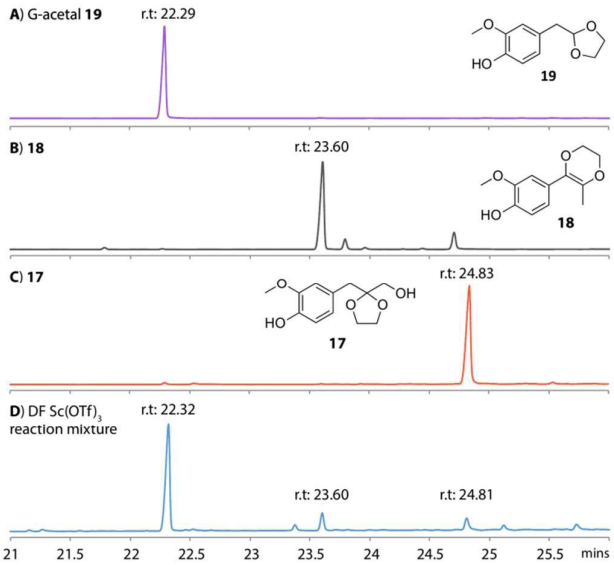

Figure 4: GC-FID traces of **A**) G-acetal **19**; **B**) semi-purified sample of **18; C) 17** and **D**) the crude reaction mixture from the DF depolymerisation with $Sc(OTf)_3$. See ESI Figures S22-S25 for full GC-FID Traces and Figures S26-S29 and Tables S8-S11 for GC-MS analysis.

Conclusions

Here we report a scalable and rapid synthetic route to the G- and S-Hibbert ketones (**1** and **2**) and the model compounds **3** and **4**. Detailed NMR analysis of **3** and **4** enabled the assignment of cross peaks corresponding to the lignin-bound Hibbert ketone structures in full for the first time. Additional studies using advanced 2D NMR techniques confirmed that when a hardwood is used as the source of lignin, both G- and S-LBHK structures are formed. This level of detailed structural assessment has not previously been carried out on the lignin-bound Hibbert ketone structures to the best of our knowledge. In addition, we have shown that it is possible to reduce the ketone functional group in the LBHK units in lignin (using 2D HSQC-TOCSY analysis) and that novel aromatic monomers **17** and **18** can be generated from lignin that contains LBHK structures. We believe this study extends significantly the current understanding of this interesting structural unit in acid-generated technical lignins.

Acknowledgements

This work was supported by EPSRC Ph.D. studentships (EP/1518175 (DMB), EP/1517938 (AN)), the Industrial Biotechnology Innovation Centre (Ph.D. studentship to DMB), CRITICAT Centre for Doctoral Training (Ph.D. studentship to IP; EP/L016419/1), EPSRC grants EP/J018139/1 and EP/K00445X/1 (SOJO) and an EPSRC Doctoral Prize Fellowship (CSL). We also acknowledge the EPSRC UK Mass Spectrometry Facility at Swansea University for mass spectrometry analysis. We would like to thank Prof. Kamer (University of St Andrews) for use of GC-MS/FID equipment, Professor Katalin Barta and Dr Reuben Carr for useful discussions.

Notes and references

§ It should be noted that both dioxasolv DF and beech lignins underwent very careful purification to remove contamination by HKs **1** and/or **2** (ESI Figures S6-S12). This is an important issue that was relatively easy to spot in our system but this is not always the case and great care should be taken to consider potential contamination with low molecular weight impurities when interpreting reaction profiles and NMR spectra.

* $Sc(OTf)_3$ would be expected to yield these results based on its Lewis acidity and hydrolysis constants. $Bi(OTf)_3$ is more acidic than $Sc(OTf)_3$ likely encouraging the subsequent conversion of **17** to dioxene **18**. In a separate experiment (ESI Scheme S8 and Figure S21) it was shown that reaction of **17** under the $Bi(OTf)_3$ conditions led to the formation of **18**. $Sc(OTf)_3$ has been reported to be on the boundary of metal triflates that can/cannot perform the previously reported lignin depolymerisation chemistry.[26b]

‡ It should be noted that the number of equivalents of $M(OTf)_x$ used in the lignin depolymerisation procedure (see ESI) were weight equivalents and there are therefore significant differences compared to the study using **1**. It cannot (at this time) be ruled out that the products **17** and **18** were generated during the cleavage of remaining consecutive β-O-4 linkages but even if this were the case it seems very likely that LBHK structures were intermediates *en*-route to their formation.

1 J. Zakzeski, P. C. a Bruijnincx, A. L. Jongerius and B. M. Weckhuysen, *Chem. Rev.*, 2010, **110**, 3552–99.
2 R. Rinaldi, R. Jastrzebski, M. T. Clough, J. Ralph, M. Kennema, P. C. A. Bruijnincx and B. M. Weckhuysen, *Angew. Chemie Int. Ed.*, 2016, **55**, 2–54.
3 P. J. Deuss, M. Scott, F. Tran, N. J. Westwood, J. G. De Vries and K. Barta, *J. Am. Chem. Soc.*, 2015, **137**, 7456–7467.
4 K. Barta, G. R. Warner, E. S. Beach and P. T. Anastas, *Green Chem.*, 2014, **16**, 191–196.
5 F. P. Bouxin, A. McVeigh, F. Tran, N. J. Westwood, M. C. Jarvis and S. D. Jackson, *Green Chem.*, 2015, **17**, 1235–1242.
6 A. McVeigh, F. P. Bouxin, M. C. Jarvis and S. D. Jackson, *Catal. Sci. Technol.*, 2016, **6**, 4142–4150.
7 J. S. Luterbacher, J. M. Rand, D. M. Alonso, J. Han, J. T. Youngquist, C. T. Maravelias, B. F. Pfleger and J. A. Dumesic, *Science.*, 2014, **343**, 277–281.
8 P. D. Sainsbury, E. M. Hardiman, M. Ahmad, H. Otani, N. Seghezzi, L. D. Eltis and T. D. H. Bugg, *ACS Chem. Biol.*, 2013, **8**, 2151–2156.
9 W. Chen, D. J. McClelland, A. Azarpira, J. Ralph, Z. Luo and G. W. Huber, *Green Chem.*, 2016, **18**, 271–281.
10 X. Zhao, K. Cheng and D. Liu, *Appl. Microbiol. Biotechnol.*, 2009, **82**, 815–827.
11 S. Van den Bosch, W. Schutyser, R. Vanholme, T. Driessen, S.-F. Koelewijn, T. Renders, B. De Meester, W. J. J. Huijgen, W. Dehaen, C. M. Courtin, B. Lagrain, W. Boerjan and B. F. Sels, *Energy Environ. Sci.*, 2015, **8**, 1748–1763.
12 M. V. Galkin and J. S. M. Samec, *ChemSusChem*, 2014, **7**, 2154–2158.
13 L. da Costa Sousa, M. Foston, V. V Bokade, A. Azarpira, F. Lu, A. Ragauskas, J. Ralph, B. E. Dale and V. Balan, *Green Chem.*, 2016, **18**, 4205-4215.
14 L. da Costa Sousa, M. Jin, S. P. S. Chundawat, V. Bokade, X. Tang, A. Azarpira, F. Lu, U. Avci, J. Humpula, N. Uppugundla,

View Article Online
DOI: 10.1039/C6OB01915C

C. Gunawan, S. Pattathil, A. M. Cheh, N. Kothari, R. Kumar, J. Ralph, M. G. Hahn, C. E. Wyman, S. Singh, B. A. Simmons, B. E. Dale and V. Balan, *Energy Environ. Sci*., 2016, **9**, 1215–1223.

15 L. Mitchell and H. Hibbert, *J. Am. Chem. Soc*., 1944, **66**, 604–607.

16 E. West, A. S. MacInnes and H. Hibbert, *J. Am. Chem. Soc*., 1943, **65**, 1187–1192.

17 M. Kulka and H. Hibbert, *J. Am. Chem. Soc*., 1943, **65**, 1180–1185.

18 H. Fisher, M. Kulka and H. Hibbert, *J. Am. Chem. Soc.,* 1944, **66**, 598–601.

19 K. Lundquist and R. Lundgren, *Acta Chem. Scand*., 1972, **26**, 2005–2023. Our synthesis of **1** and **2** differs from that of Lundquist in that we use a much shorter sequence to access the precursor triol. In our case this is achieved through the use of a TBS-protecting group in contrast to Lundquist who prepares **1** and **2** from the unprotected triol precursor. See also for synthesis of unprotected triol: E. Adler and B. Gustafsson, *Acta Chem. Scand.* 1963, **17**, 27-36.

20 L. Mitchell and H. Hibbert, *J. Am. Chem. Soc*., 1944, **66**, 602–604.

21 S. Constant, H. L. J. Wienk, A. E. Frissen, P. de Peinder, R. Boelens, D. S. van Es, R. J. H. Grisel, B. M. Weckhuysen, W. J. J. Huijgen, R. J. A. Gosselink and P. C. A. Bruijnincx, *Green Chem*., 2016, **18**, 2651–2665.

22 A. Brandt, L. Chen, B. E. van Dongen, T. Welton and J. P. Hallett, *Green Chem*., 2015, **17**, 5019–5034.

23 C. S. Lancefield and N. J. Westwood, *Green Chem*., 2015, **17**, 4980–4990.

24 V. Dalla and J. P. Catteau, *Tetrahedron*, 1999, **55**, 6497–6510.

25 A. Rahimi, A. Ulbrich, J. J. Coon and S. S. Stahl, *Nature*, 2014, **515**, 249–252.

26 a) C. W. Lahive, P. J. Deuss, C. S. Lancefield, Z. Sun, D. B. Cordes, C. Young, F. Tran, A. M. Z. Slawin, J. G. de Vries, P. C. J. Kamer, N. J. Westwood and K. Barta, *J. Am. Chem. Soc*., 2016, **138**, 8900–8911; b) P. Deuss, C. W. Lahive, C. S. Lancefield, N. J Westwood, P. C. J. Kamer, K. Barta, J. G. de Vries, *ChemSusChem*., 2016, *Manuscript in Press*.

27 C. S. Lancefield, O. S. Ojo, F. Tran and N. J. Westwood, *Angew. Chem. Int. Ed. Engl*., 2015, **127**, 260-264**.**

28 CCDC 1500178 (**1**) and 1500179 (**2**) contain the supplementary crystallographic data for this paper. These data can be obtained free of charge from The Cambridge Crystallographic Data Centre via www.ccdc.cam.ac.uk/data_request/cif.

29 W. Boerjan, J. Ralph and M. Baucher, *Annu. Rev. Plant Biol*., 2003, **54**, 519–546.

30 L. Zhang and G. Gellerstedt, *Magn. Reson. Chem*., 2007, **45**, 37–45.